Range-Doppler Division Multiple Access for Joint Radar and Communication

Adham Sakhnini*†, André Bourdoux†, Sofie Pollin*†
*Department of Electrical Engineering, KU Leuven, Belgium
†IMEC, Kapeldreef 75, 3001 Leuven, Belgium

***Abstract*—This paper presents a multiple-access procedure for joint radar and communication systems. Dedicated radar antennas transmit uplink pilots in the same time-frequency resources as the user pilots over several coherence blocks. The radar and communication channels are subsequently estimated wherein the respective systems proceed as conventional. In order to facilitate pilot reuse and mitigate interchannel interference, the radar and user pilots are modulated in time and frequency so that the channels are orthogonal in the range-Doppler domain. This allows the respective channels to be separated without mutual interference or the need to allocate dedicated radar pilots. The main advantage is the time-division duplex compatibility and the near optimal radar performance. The performance trade-offs are discussed and the method is demonstrated with numerical simulations, demonstrating a relatively unaffected EVM while simultaneously recovering the radar channel for sensing.**

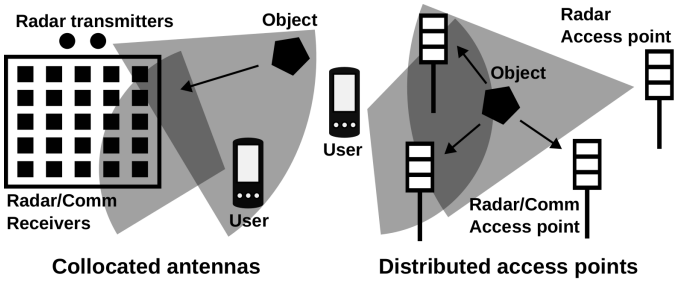

Fig. 1: Virtual uplink radar and communications in collocated (e.g., cellular) and distributed (e.g., cell-free) systems. The radar and users transmit in the same time and frequency resources in the uplink and are then separated and processed conventionally at the receivers.

I. Introduction

Integrating radar functionalities into wireless communication systems has emerged as a potential technology in future communication standards [1]–[3], with a substantial interest being currently expressed from industry [4]–[6]. The integration seeks to exploit the environmental awareness to improve spectrum utilization and enable new services, such as environmental sensing and surveillance, without deploying any new hardware. The vision is also to improve the actual communication system, where some current research is focusing on blockage mitigation, beam training and physical layer security by making use of the sensing modality [7].

From a practical point of view, the main challenge is to integrate the radar into the same hardware platform and infrastructure at the smallest cost and system loss possible. At the same time, the radar needs to maintain sufficient performance to meet the demanding use cases being promised, such as operating in urban environments, which are challenging even for state of the art radar systems (see e.g., [8]).

In this paper, we consider a *virtual uplink* radar integration as presented in [9] for cellular systems and in [10], [11] for cell-free systems. The setup is illustrated in Fig. 1 and operates in the uplink by scheduling dedicated radar transmitters to illuminate the environment in the same time-frequency resources as the user communication signals. The radar transmitters may be collocated with the communication receivers (using e.g., the downlink transmit antennas), or distributed as individual access points being scheduled for radar transmission. The task of the receivers is to separate the radar echoes from communication signals using e.g., interference cancellation [9], [10] or power control [11]. After separation, the radar and communication systems proceed as conventional.

In contrast to other integrations that realize the radar in the spatial domain with transmit beamforming [12], [13] or with downlink and uplink communication waveforms [14], the proposed approach benefits from a constant and uniform illumination, which maintains the detection performance and increases the Doppler sensitivity and unambiguous region. In addition, the need to consider (possibly unknown) precoders and data modulations is circumvented by utilizing dedicated radar signals. Furthermore, the need for in-band full-duplex may be potentially alleviated through antenna isolation (as discussed in [9]), and synchronization between the antennas may in principle be resolved by the infrastructure. The key disadvantage is the need for dedicated radar transmitters and the need to mitigate the associated cross interference between the radar and communication signals.

In this paper, we present a multiple access procedure in the range-Doppler domain for radar and multi-user communications. The method is based on the range and Doppler domain multiple-input multiple-output (MIMO) radar principle [15]–[17] and is illustrated in Fig. 2 for the case of a time-division duplex (TDD) frame structure. The principle is to estimate the radar and user channels in a shared uplink training phase. By modulating the pilots over several coherence blocks and TDD frames, it becomes possible to separate the pilots in the range-Doppler domain, hence avoiding communication interference in the radar system and pilot contamination from the radar pilots in the communication system.

As shown in the paper, the key advantage is the high

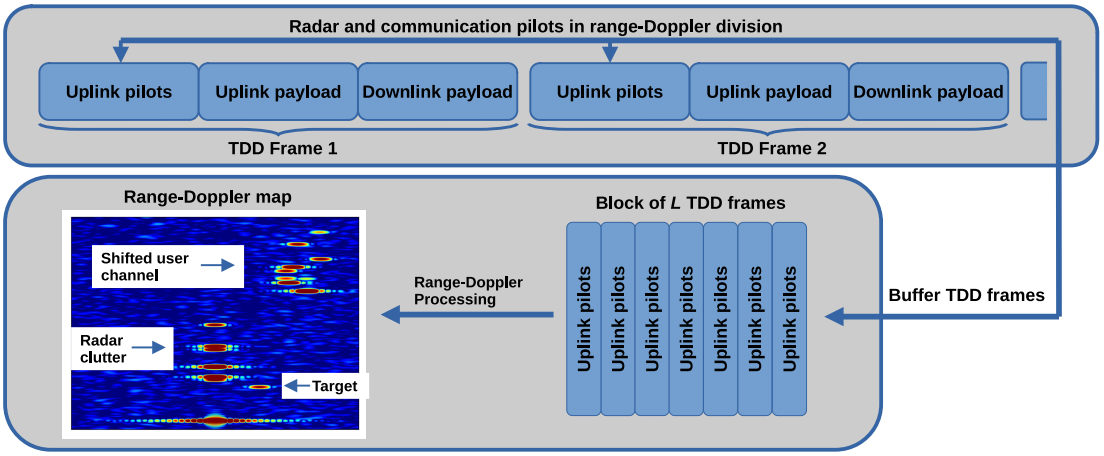

Fig. 2: The range-Doppler division multiple access procedure presented in this paper. The radar and users transmit pilots that are modulated over a several TDD frames so that the radar and user channels can be separated in the range-Doppler domain.

isolation between radar and user pilots, in particular when compared to code-domain multiple access, and the potential to not add any overhead in terms of longer pilot sequences to the communication system. We present the signal model and show that conventional pilot spreading is infeasible to the radar system due to false detections caused by the cross-interference from the communication system. We then present the range-Doppler division multiple access procedure, discuss the trade-offs in radar and communication performance and demonstrate the concept with examples and numerical simulations.

II. Signal model

For the ease of presentation and without loss of generality, we consider a single radar transmitter, communication receiver and communication transmitter (i.e., user). An extension to multiple transmitters, receivers and users follows by direct superposition and is therefore omitted. Furthermore, we use the orthogonal frequency division multiplexing (OFDM) waveform, although we emphasize that the method can also be used with other waveforms with only few modifications.

The frame structure is illustrated in Fig. 2 and consists of a radar and communication channel estimation phase and a downlink and uplink data transmission phase. The channel coefficients for the radar and user are assumed to be estimated in blocks of K_t subcarriers and L_t symbols. We let a frame consist of K blocks of K_t subcarriers and L time-division duplex frames (TDD) which the radar integrates over. The subcarrier spacing is denoted as Δf, the symbol duration (including the cyclic prefix) is denoted as T_{ofdm} and the TDD frame duration is denoted as T_{tdd}.

In the following, we let i and j denote the subcarriers and symbols within a training block used for channel estimation, while k and l denotes the block of subcarriers and the TDD frame, respectively. The demodulated OFDM signal (in the frequency domain) is given by

$$y_{i,j}(k,l) = y^{(r)}_{i,j}(k,l) + y^{(u)}_{i,j}(k,l) + n_{i,j}(k,l) \tag{1}$$

where $n_{i,j}(k,l)$ is additive noise, and

$$y^{(x)}_{i,j}(k,l) = \sum_{q=1}^{Q_x} \alpha^{(x)}_q s^{(x)}_{i,j} e^{j2\pi\Delta f \tau^{(x)}_q (K_t k + i)} \tag{2}$$

$$\times\, e^{-j2\pi f^{(x)}_{D,q}(T_{\text{tdd}} l + T_{\text{ofdm}} j)} \tag{3}$$

is the received user and radar signals, where $x = u$ represents the user and $x = r$ the radar. The complex valued amplitude of the q:th path is denoted as $\alpha^{(x)}_q$, where Q_x denotes the total number of paths. The corresponding time delays are denoted as $\tau^{(x)}_q$ and the Doppler shifts as $f^{(x)}_{D,q}$. Note that the time delays also account for synchronization errors, assuming they do not extend the cyclic prefix length.

The pilot sequences are given by $s^{(x)}_{i,j}$ and are (initially) designed to be mutually orthogonal and have unit power:

$$\sum_{i=1}^{K_t}\sum_{j=1}^{L_t} |s^{(x)}_{i,j}|^2 = 1, \quad \sum_{i=1}^{K_t}\sum_{j=1}^{L_t} s^{(u)}_{i,j}\bar{s}^{(r)}_{i,j} = 0 \tag{4}$$

where the overline $\bar{(\cdot)}$ represents the complex conjugate. The assumption of orthogonal pilots will be dropped later. We assume that the same pilot $s^{(x)}_{i,j}$ is used in every block of subcarriers and symbols across the TDD frames. This prevents the decorrelation of user signals in the subsequent range-Doppler processing, which (as will be shown) allows the system to separate the radar and communication signals. A concern may be that the peak to average power ratio (PAPR) increases due to the repetitions in the frequency domain. However, this can be significantly reduced by scrambling all $s^{(x)}_{i,j}$ prior to transmission with a common scrambler.

A. Radar channel estimation

We estimate the radar channel by direct despreading. Other estimators such as the minimum mean squared error (MMSE) estimator can also be used in the case of multiple antennas and available large scale fading statistics [18].

The estimated radar channel $h^{(r)}(k,l)$ is given as

$$h^{(r)}(k,l) = \sum_{i=1}^{K_t} \sum_{j=1}^{L_t} y_{i,j}(k,l) \bar{s}_{i,j}^{(r)}(k,l) \tag{5}$$

where the double sum despreads the channels. By expanding $y_{i,j}(k,l)$ into the radar, user and noise components, we get

$$h^{(r)}(k,l) = g_r^{(r)}(k,l) + g_r^{(u)}(k,l) + n(k,l) \tag{6}$$

where $g_r^{(r)}(k,l)$ is radar channel, $g_r^{(u)}(k,l)$ is the *co-channel interference* originating from the user and $n(k,l)$ is the resulting noise. The channel components can be expressed as

$$g_r^{(x)}(k,l) = \sum_{q=1}^{Q_x} \beta_{r,q}^{(x)} e^{j2\pi\Delta f \tau_q^{(x)} K_t k} e^{-j2\pi f_{D,q}^{(x)} T_{\text{tdd}} l} \tag{7}$$

where the amplitudes $\beta_{r,q}^{(x)}$ are given by

$$\beta_{r,q}^{(x)} = \alpha_q^{(x)} \sum_{i=1}^{K_t} \sum_{j=1}^{L_t} s_{i,j}^{(x)} \bar{s}_{i,j}^{(r)} e^{j2\pi\Delta f \tau_q^{(x)} i} e^{-j2\pi f_{D,q}^{(x)} T_{\text{ofdm}} j} \tag{8}$$

and represent the quality of the radar channels estimates. Note that $\beta_{r,q}^{(r)} = \alpha_q^{(r)}$ and $\beta_{r,q}^{(u)} = 0$ when $\tau_q^{(x)} = 0$ and $f_{D,q}^{(x)} = 0$, which implies that 1) the radar channel can be perfectly estimated and 2) the user interference is perfectly rejected.

In general, we have that $\beta_{r,q}^{(u)} \neq 0$ when $f_{D,q}^{(u)} \neq 0$ and $\tau_q^{(u)} \neq 0$, which implies that the pilot sequences $s_{i,j}^{(r)}$ and $s_{i,j}^{(u)}$ are non-orthogonal at the receiver due to the channel impairments, *even if they were originally designed to be orthogonal at the transmitter*. Although the power of $\beta_{r,q}^{(u)}$ can be several orders of magnitude smaller than $\alpha_q^{(u)}$, the corresponding interference may still be several decibel above the noise floor after radar processing (this is shown in Section IV). The consequence is that the radar must raise the detection threshold in order to maintain a constant false alarm rate, which reduces the maximum detectable distance. This implies that optimal radar performance cannot always be maintained by allocating orthogonal pilots between the radar and communication system due to the detection loss.[1]

B. Range-Doppler processing

The radar performs range-Doppler processing based on the channel estimates $h^{(r)}(k,l)$. In particular, a filter $w(k,l;\tau,f_D)$ is constructed to match an echo with time delay τ and Doppler shift f_d. The delay-Doppler map is obtained by evaluating

$$\chi(\tau,f_D) = \sum_{k=1}^{K} \sum_{l=1}^{L} h^{(r)}(k,l) \bar{w}(k,l;\tau,f_D) \tag{9}$$

over a grid of delays and Doppler shifts. The corresponding (monostatic) range-Doppler map is obtained by the mapping $d = 0.5\tau c$, where c is the speed of light. A common choice of $w(k,l;\tau,f_D)$ is the matched filter, which is given as

$$w_{\text{mf}}(k,l;\tau,f_D) = e^{j2\pi\Delta f \tau K_t k} e^{-j2\pi f_D T_{\text{tdd}} l} \tag{10}$$

[1]This is also the case when the user is decorrelated by randomizing the pilots in time and frequency, depending on the delays and Doppler shifts.

and often implemented as a windowed two dimensional fast Fourier transform (FFT). Note that the processing gain is same for the radar and the co-channel interference since the signal structure is the same (cf., (7)).

III. Range-Doppler domain multiple access

The frame structure of a communication system is often specified by the standard and designed for worst case scenarios, which implies redundancy in many use cases. In particular, if the delay and Doppler spread is sufficiently small, then a portion of the range-Doppler space can be used to establish orthogonality between the radar and users, without allocating any dedicated pilots. This provides a spectrally efficient way of integrating the radar into the training segment.

A. The multiple access procedure

In the following, we let τ_{max} and f_{max} denote the maximum path delay and Doppler shift of the radar and the communication system, and $\Delta\tau_{\text{sync}}$ denote largest synchronization error of the user. By shifting the radar by $\tau_{\text{max}} + \Delta\tau_{\text{sync}}$ in range and f_{max} in Doppler, it can be guaranteed that the radar channel does not overlap with the user channel (provided sufficient range-Doppler area). The orthogonality can then be established by applying a true time delay and Doppler shift to the radar pilot at transmission. However, it is more advantageous to directly modify the pilot sequence in the digital domain as

$$s_{i,j}^{(x)}(k,l) = \begin{cases} s_{i,j}^{(u)} & x = u \\ s_{i,j}^{(r)} \phi^{(r)}(k,l) & x = r \end{cases} \tag{11}$$

where $\phi^{(r)}(k,l)$ is a linear phase ramp given by

$$\phi^{(r)}(k,l) = e^{j2\pi K_t \Delta f (\tau_{\text{max}} + \Delta\tau_{\text{sync}}) k} e^{-j2\pi f_{\text{max}} T_{\text{tdd}} l} \tag{12}$$

which applies the phase shifts over blocks of subcarriers and TDD frames. Note that the digital modulation does not affect the coherence time or bandwidth, and does not cause intersymbol or intercarrier interference when exceeding the cyclic prefix duration or the subcarrier spacing. Therefore, the channel model (6) is still valid, yielding

$$h^{(r)}(k,l) = g_r^{(r)}(k,l)\phi^{(r)}(k,l) + g_r^{(u)}(k,l) + n(k,l) \tag{13}$$

which allows the communication channel to be separated from the radar channel by lowpass filtering $h^{(r)}(k,l)$ as

$$\hat{h}^{(r)}(k,l) = \text{LPF}\{h^{(r)}(k,l)\bar{\phi}^{(r)}(k,l)\} \tag{14}$$

which gives the radar channel estimate

$$\hat{h}^{(r)}(k,l) \approx g_r^{(r)}(k,l) + e(k,l) \tag{15}$$

where $e(k,l) = \text{LPF}\left\{n(k,l)\bar{\phi}^{(r)}(k,l)\right\}$ is the resulting additive noise. Once the channel is recovered, the system proceeds with conventional radar signal processing.

B. Recovering the communication channel

If the user and radar have orthogonal pilots, then user signal processing proceeds as in conventional communication systems. However, it is possible to save resources by assigning the same pilot to each entity and then recovering the user channel by exploiting the division in the range-Doppler domain. This can be done by filtering out the radar channel, analogously to the radar case (cf. (14)), or by employing parametric channel estimation techniques (see e.g., [19]), where the channel is constructed from components with delays and Doppler shifts within the allocated range-Doppler area.

C. Trade-off analysis

In the following, we quantify the losses associated with the multiple access procedure when assuming a pilot reuse. We stress that an extension to multiple radars, receivers and users is straightforward and is therefore left out.

a) Coherence bandwidth and delay spread: We divide the delay (i.e., range) domain into two parts in order to accommodate the delay spread of the user and radar channels. The user is allocated a portion of length $\tau_{\max} + \Delta\tau_{\text{sync}}$ and the radar a portion with length $\tau_{\max}$. Therefore, in order to prevent aliasing in the range-domain, the maximum unambiguous delay is obtained from the condition

$$K_t \Delta f \left(2\tau_{\max} + \tau_{\text{sync}}\right) = 1 \tag{16}$$

which gives

$$\tau_{\max} = \frac{1}{2}\left(\frac{1}{K_t \Delta f} - \Delta\tau_{\text{sync}}\right) \tag{17}$$

where $1/(K_t\Delta f) > \Delta\tau_{\max}$ is an underlying assumption (i.e., the users are able to synchronize properly). Note that $K_t\Delta f$ corresponds to the assumed coherence bandwidth, which affects the pilot overhead and hence the spectral efficiency.

As can be seen from (17), there is a direct trade-off between radar and communications, where the communication system prefers the largest possible coherence bandwidth (i.e., $K_t\Delta f$), while the radar prefers the largest possible unambiguous delay (i.e., $\tau_{\max}$). Therefore, for dynamic frame structures, the radar comes at the cost of pilot overhead, because any redundancy in $\tau_{\max}$ implies that the coherence bandwidth $K_t\Delta f$ could have been increased. On the other hand, for systems with fixed frame structures, the redundancy in delay spread can be viewed as an opportunity to schedule radar transmitters without incurring any performance losses.

b) Coherence time and mobility: We divide the Doppler domain into two parts, one for the user and one for the radar. If the maximum Doppler shift is $\pm f_{\max}$, then the total range of Doppler shifts becomes $4f_{\max}$. Therefore, in order to prevent aliasing, the maximum Doppler shift becomes

$$f_{\max} = \frac{1}{4T_{\text{tdd}}} \tag{18}$$

which comprises a trade-off in pilot overhead (i.e., large T_{tdd}) and maximum mobility supported (i.e., $f_{\max}$). Note that in the case of only a single user, it holds that $f_{\max} = 1/(2T_{\text{tdd}})$, which corresponds to the maximum mobility when compared to allocating a radar transmitter. Hence, the maximum mobility that the system can support is reduced when scheduling radar transmitters in Doppler division.

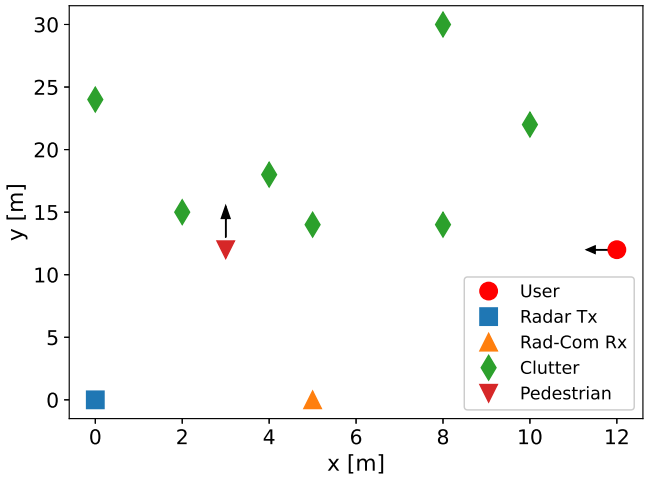

Fig. 3: The simulation setup, consisting of a radar transmitter (Tx), radar and communication receiver (Rx), a user and $7+1$ point scatterers resembling clutter and a pedestrian.

It is worth nothing that for the considered special case of one radar, the coherence time (as defined in [18] and [20]) coincides with T_{tdd} for the maximum Doppler shift $f_{\max}$ in (18). This implies that if the communication system is designed to meet a mobility by using that coherence time expression, then there is no loss in performance.

c) Latency: When dividing the radar and user in the Doppler domain, the method requires blockwise processing over several TDD frames in order to separate the respective channels. This has the drawback of increasing the latency of the communication system, which represents a significant system loss. This loss may potentially be reduced with recursive filtering and channel estimation techniques.

IV. Numerical demonstration

A. Simulation setup

We consider a radar and communication system with the parameters shown in Table I. The system operates at the 28 GHz carrier frequency and uses the OFDM waveform with $KK_t = 3200$ subcarriers and $\Delta f = 183$ kHz, corresponding to a bandwidth of 586 MHz. The TDD duration is $T_{\text{tdd}} = 0.2$ ms and the pilots are spread over $K_t = 8$ subcarriers and $L_t = 4$ symbols, providing $K_tL_t = 32$ orthogonal sequences and a coherence bandwidth of $K_t\Delta f = 1.46$ MHz.

The scenario is illustrated in Fig 3 and consists of a radar transmitter (Tx) and a radar and communication receiver (Rx) mounted at a 2 m height, and a mobile user with velocity $(10, 0, 0)$ m/s. The user is modeled to have a 64 ns timing offset. The clutter is modeled using 7 static point scatterers with a radar cross section (RCS) ranging from 10 to 25 dBsm. A point scatterer with velocity $(0, -5, 0)$ m/s is used to model

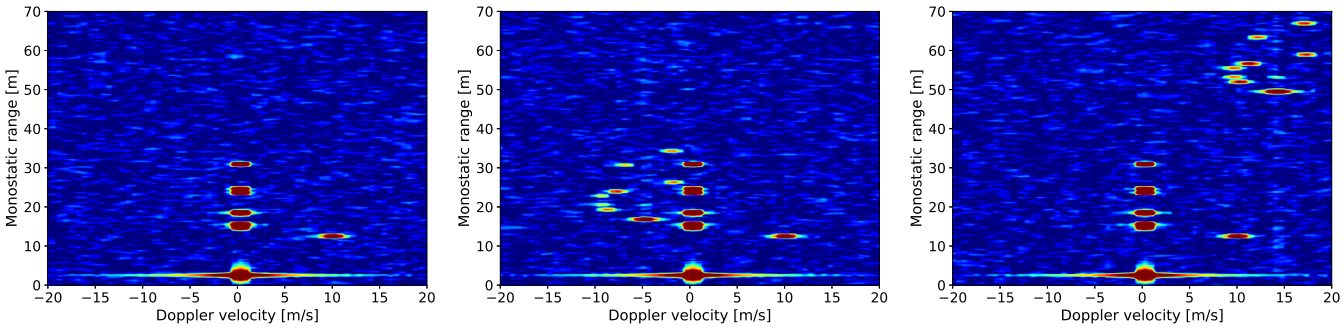

(a) Radar only (b) User + Radar (orthogonal pilots) (c) User + Radar$^{(*)}$

Fig. 4: Comparison of range-Doppler maps with and without user interference. $^{(*)}$Non-orthogonal pilots and shifting.

TABLE I: Simulation parameters.

Parameter	Notation	Value	Unit
Carrier frequency	-	28	GHz
Transmit power	-	20	dBm
Antenna gain	-	4	dBi
Noise figure		15	dB
Number of subcarriers	KK_t	3200	-
No. training subcarriers	K_t	8	-
Subcarrier spacing	Δf	183	kHz
No. payload symbols	-	30	-
No. training symbols	L_t	4	-
No. TDD frames	L	96	-
Symbol duration	T_{ofdm}	5.85	us
TDD frame duration	T_{tdd}	0.2	ms

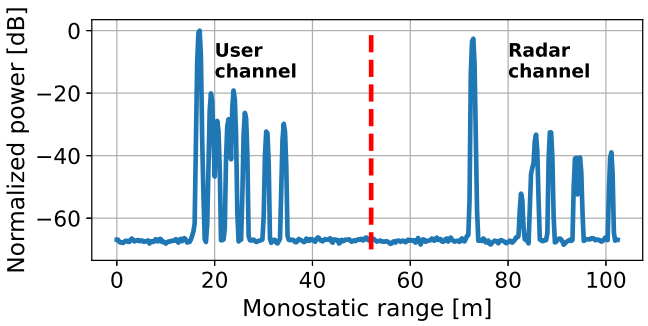

Fig. 5: Illustration of a range-division multiple access.

a pedestrian with 0 dBsm RCS. The direct path amplitudes are modeled with Friis formula [21] and the reflections with the radar range equation [22], with the phases being random.

The received data is processed by buffering the TDD frames and demodulating the respective OFDM symbols. The channels are then estimated by direct de-spreading and used to equalize the impairments in the uplink payloads. Orthogonal pilots are generated using the singular value decomposition (SVD) and non-orthogonal pilots by sampling random complex Gaussian vectors. A common binary scrambler is applied to all pilots in order to reduce the PAPR.

B. Radar analysis

The range-Doppler maps obtained after radar channel estimation are shown in Fig. 4, where the color scale is in decibel ranging from the noise floor and 40 dB above. The case without any user is illustrated in Fig. 4a, showing the strong direct path component and clutter at zero Doppler and the pedestrian at 10 m/s Doppler velocity (the velocity is doubled due to the two-path propagation and the sign is flipped by convention). Fig. 4b shows the range-Doppler map when a radar and user are transmitting orthogonal pilots. As can be seen, the user channel leaks into the range-Doppler map and gives rise to false peaks even though the pilots are orthogonal. This is due to the impairments caused by the delays and Doppler shifts, as captured by (8). The line of sight and strongest multipath component are measured to 52 and 37 dB above the noise floor (the processing gain is $10\log_{10}(KL) = 46$ dB), which represents a significant multiple access loss in the radar system. Fig. 4c illustrates the same range-Doppler map when using non-orthogonal pilots and after digitally shifting the radar channel away from the user channel by 70 m in range and 19 m/s in Doppler velocity. As can be seen, the user interference is still present (and is in fact stronger due to the pilots), but does not overlap with the radar channel. This allows the radar to operate optimally within the allocated range-Doppler area by rejecting the false detections based on the range and Doppler velocity.

C. Communication analysis

In the following, we have locked the seed of all simulations so that the same channel and waveform is used. In order to demonstrate the performance with non-orthogonal pilots, we separate the channels in the range-Doppler domain and then blank the radar channel. This is illustrated in Fig. 5 in the range-domain, where the red line separates the channel, hence allowing the radar taps to blanked.

Fig. 6 illustrates the QPSK constellations obtained from randomly sampling the equalized subcarriers in the uplink payload. Fig. 6a shows the case with only a user and Fig. 6b the case with a radar and user when using orthogonal pilots. As can be seen, the performance is similar, corresponding to error vector magnitude (EVM) values of 21.13 and 21.44

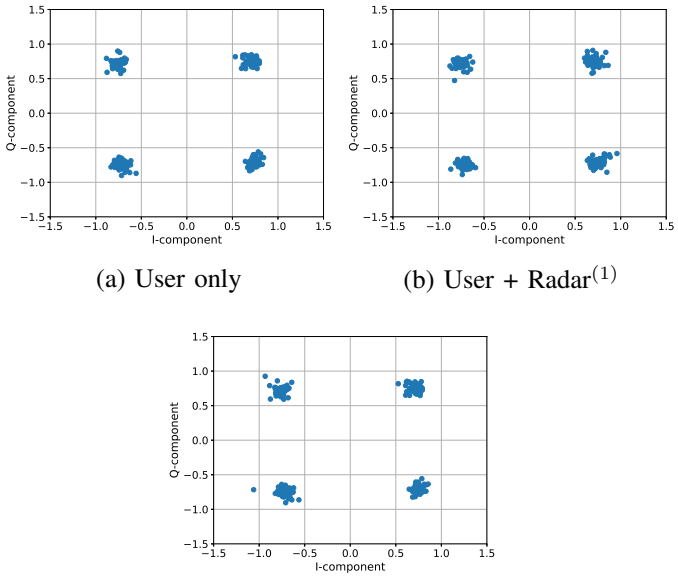

(a) User only

(b) User + Radar$^{(1)}$

(c) User + Radar$^{(2)}$

Fig. 6: Comparison of QPSK constellations.$^{(1)}$With orthogonal pilots. $^{(2)}$With non-orthogonal pilots and channel blanking.

TABLE II: Measured EVMs. $^{(1)}$with orthogonal pilots. $^{(2)}$with non-orthogonal pilots and range-Doppler domain blanking.

Scenario	Average EVM	Unit
User only	22.13	dB
User + Radar$^{(1)}$	21.44	dB
User + Radar$^{(2)}$	21.70	dB

dB, as shown in Table II. The similar performance is because the scenario corresponds to conventional channel estimation in code division, where the radar acts as a *virtual user*. Fig. 6c shows the constellation obtained after shifting and blanking the radar channel in the range-Doppler domain, using non-orthogonal pilots. As can be seen, the performance remains largely unchanged, with an EVM measured to 21.70 dB. These results show that the range-Doppler domain provides an efficient way of integrating the radar system.

V. Conclusion

This paper has presented a multiple-access procedure for radar and communications. The method operates in the training phase by modulating the radar and communication pilots to be orthogonal in the range-Doppler domain. This allows the channels to be separated without mutual interference or the need to allocate dedicated pilots to the radar system. The performance trade-offs are discussed and the effectiveness of the method is demonstrated with numerical simulations, where we show that the radar can operate with near-optimal performance and negligible impact on the communications.

References

[1] C. De Lima and et al., "Convergent Communication, Sensing and Localization in 6G Systems: An Overview of Technologies, Opportunities and Challenges," *IEEE Access*, vol. 9, pp. 26 902–26 925, 2021.

[2] T. Wild, V. Braun, and H. Viswanathan, "Joint Design of Communication and Sensing for Beyond 5G and 6G Systems," *IEEE Access*, vol. 9, pp. 30 845–30 857, 2021.

[3] H. Wymeersch, D. Shrestha, C. M. de Lima, V. Yajnanarayana, B. Richerzhagen, M. F. Keskin, K. Schindhelm, A. Ramirez, A. Wolfgang, M. F. de Guzman, K. Haneda, T. Svensson, R. Baldemair, and S. Parkvall, "Integration of Communication and Sensing in 6G: a Joint Industrial and Academic Perspective," in *2021 IEEE 32nd Annual International Symposium on Personal, Indoor and Mobile Radio Communications (PIMRC)*, 2021, pp. 1–7.

[4] VDE, "Joint communication and sensing," Press Release, December 2021. [Online]. Available: https://www.vde.com/en/press/press-releases/joint-communication-and-sensing

[5] H. Andersson, "Joint communication and sensing in 6g networks," Ericsson Blog, 2021. [Online]. Available: https://www.ericsson.com/en/blog/2021/10/joint-sensing-and-communication-6g

[6] Huawei Technology Insights, "6G: The Next Horizon White Paper," 2022. [Online]. Available: https://www.huawei.com/en/technology-insights/future-technologies/6g-white-paper

[7] F. Liu, Y. Cui, C. Masouros, J. Xu, T. X. Han, Y. C. Eldar, and S. Buzzi, "Integrated sensing and communications: Toward dual-functional wireless networks for 6g and beyond," vol. 40, no. 6, pp. 1728–1767.

[8] I. Bilik, O. Longman, S. Villeval, and J. Tabrikian, "The rise of radar for autonomous vehicles: Signal processing solutions and future research directions," vol. 36, no. 5, pp. 20–31.

[9] M. Temiz, E. Alsusa, and M. W. Baidas, "A Dual-Function Massive MIMO Uplink OFDM Communication and Radar Architecture," *IEEE Transactions on Cognitive Communications and Networking*, pp. 1–1, 2021.

[10] A. Sakhnini, M. Guenach, A. Bourdoux, H. Sahli, and S. Pollin, "A Target Detection Analysis in Cell-Free Massive MIMO Joint Communication and Radar Systems," in *2022 IEEE International Conference on Communications (ICC): Mobile and Wireless Networks Symposium (IEEE ICC'22 - MWN Symposium)*, May 2022.

[11] A. Sakhnini, A. Bourdoux, M. Guenach, H. Sahli, and S. Pollin, "Uplink payload power control in Cell-Free communication and radar networks," in *2022 IEEE Global Communications Conference: Mobile and Wireless Networks (Globecom 2022 MWN)*.

[12] F. Liu, C. Masouros, A. Li, H. Sun, and L. Hanzo, "MU-MIMO Communications With MIMO Radar: From Co-Existence to Joint Transmission," *IEEE Transactions on Wireless Communications*, vol. 17, no. 4, pp. 2755–2770, apr 2018.

[13] F. Liu, C. Masouros, A. P. Petropulu, H. Griffiths, and L. Hanzo, "Joint Radar and Communication Design: Applications, State-of-the-Art, and the Road Ahead," *IEEE Transactions on Communications*, vol. 68, no. 6, pp. 3834–3862, jun 2020.

[14] D. K. Pin Tan, J. He, Y. Li, A. Bayesteh, Y. Chen, P. Zhu, and W. Tong, "Integrated sensing and communication in 6g: Motivations, use cases, requirements, challenges and future directions," in *2021 1st IEEE International Online Symposium on Joint Communications & Sensing (JC&S)*, pp. 1–6.

[15] A. Bourdoux, U. Ahmad, D. Guermandi, S. Brebels, A. Dewilde, and W. Van Thillo, "Pmcw waveform and mimo technique for a 79 ghz cmos automotive radar," in *2016 IEEE Radar Conference (RadarConf)*, pp. 1–5.

[16] F. Jansen, "Automotive radar doppler division mimo with velocity ambiguity resolving capabilities," in *2019 16th European Radar Conference (EuRAD)*, pp. 245–248.

[17] Y. Sun, M. Bauduin, and A. Bourdoux, "Enhancing unambiguous velocity in doppler-division multiplexing mimo radar," in *2021 18th European Radar Conference (EuRAD)*, pp. 493–496.

[18] Özlem Tuğfe Demir, E. Björnson, and L. Sanguinetti, "Foundations of User-Centric Cell-Free Massive MIMO," Aug. 2021.

[19] Y. Liu, Z. Tan, H. Hu, L. J. Cimini, and G. Y. Li, "Channel Estimation for OFDM," vol. 16, no. 4, pp. 1891–1908.

[20] D. Tse and P. Viswanath, *Fundamentals of Wireless Communication*. Cambridge University Press, 2005.

[21] A. Molisch, *Wireless Communications*. John Wiley & Sons, 2010.

[22] M. Richards, *Fundamentals of Radar Signal Processing, Second Edition*. McGraw-Hill Education, 2014.